N-Linked Glycosylation of the Hemagglutinin Protein Influences Virulence and Antigenicity of the 1918 Pandemic and Seasonal H1N1 Influenza A Viruses

Xiangjie Sun,[a] Akila Jayaraman,[c] Pavithra Maniprasad,[c] Rahul Raman,[c] Katherine V. Houser,[a,b] Claudia Pappas,[a] Hui Zeng,[a] Ram Sasisekharan,[c] Jacqueline M. Katz,[a] Terrence M. Tumpey[a]

Immunology and Pathogenesis Branch, Influenza Division, National Center for Immunology and Respiratory Diseases, Centers for Disease Control and Prevention, Atlanta, Georgia, USA[a]; Graduate Program in Immunology and Molecular Pathogenesis of the Graduate Division of Biological and Biomedical Sciences, Emory University, Atlanta, Georgia, USA[b]; Harvard-MIT Division of Health Sciences and Technology, Singapore-MIT Alliance for Research and Technology, Department of Biological Engineering, Koch Institute for Integrative Cancer Research, Massachusetts Institute of Technology, Cambridge, Massachusetts, USA[c]

The hemagglutinin (HA) protein is a major virulence determinant for the 1918 pandemic influenza virus; however, it encodes no known virulence-associated determinants. In comparison to seasonal influenza viruses of lesser virulence, the 1918 H1N1 virus has fewer glycosylation sequons on the HA globular head region. Using site-directed mutagenesis, we found that a 1918 HA recombinant virus, of high virulence, could be significantly attenuated in mice by adding two additional glycosylation sites (asparagine [Asn] 71 and Asn 286) on the side of the HA head. The 1918 HA recombinant virus was further attenuated by introducing two additional glycosylation sites on the top of the HA head at Asn 142 and Asn 172. In a reciprocal experimental approach, deletion of HA glycosylation sites (Asn 142 and Asn 177, but not Asn 71 and Asn 104) from a seasonal influenza H1N1 virus, A/Solomon Islands/2006 (SI/06), led to increased virulence in mice. The addition of glycosylation sites to 1918 HA and removal of glycosylation sites from SI/06 HA imposed constraints on the theoretical structure surrounding the glycan receptor binding sites, which in turn led to distinct glycan receptor binding properties. The modification of glycosylation sites for the 1918 and SI/06 viruses also caused changes in viral antigenicity based on cross-reactive hemagglutinin inhibition antibody titers with antisera from mice infected with wild-type or glycan mutant viruses. These results demonstrate that glycosylation patterns of the 1918 and seasonal H1N1 viruses directly contribute to differences in virulence and are partially responsible for their distinct antigenicity.

Among the 17 known hemagglutinin (HA) subtypes and 9 known neuraminidase (NA) subtypes of influenza A viruses, only three subtypes (H1N1, H2N2, and H3N2) have adapted successfully to infect and transmit efficiently among humans (1). The influenza A virus subtype H1N1 was responsible for the most devastating pandemic in recorded history, resulting in an estimated 20 to 50 million worldwide deaths in 1918 (2). Following the 1918 pandemic, the H1N1 influenza virus continued to circulate in humans, causing annual epidemics with the exception of years 1957 to 1977, in which the H2N2 and H3N2 viruses emerged in humans to become the dominant subtypes (3). Unlike seasonal influenza, in which infection usually causes only mild respiratory symptoms in most healthy adults, the 1918 virus caused severe respiratory illness with high mortality rates (4, 5). In particular, mortality rates were high among healthy adults 15 to 34 years old, an age group not usually associated with severe illness or death from influenza (5). In 2009, a novel influenza A H1N1 virus [A(H1N1)pdm09] emerged in humans and spread throughout the world, resulting in the declaration of a pandemic by the World Health Organization (WHO) (6). During the subsequent winter seasons, the A(H1N1)pdm09 virus continued to circulate throughout the world and appears to have replaced the seasonal H1N1 virus (7).

It has been demonstrated previously that the HA gene is a major determinant for the high virulence of the 1918 virus (8, 9). In particular, among the eight 1918 gene segments studied, only the HA gene was able to confer a virulent phenotype in mice when rescued on the genetic background of avirulent human influenza viruses. The HA protein is a homotrimer of approximately 200

kDa and is synthesized as a polypeptide HA0 that is posttranslationally cleaved into two subunits, HA1 and HA2. HA0 cleavage is essential for viral infectivity, pathogenicity, and spread of the virus in the infected host (10). The presence of polybasic amino acids at the cleavage site of HA is a major virulence determinant of highly pathogenic avian influenza viruses (subtype H5 and H7) facilitating systemic spread and lethal disease in poultry and mammals (11). The 1918 virus does not possess the typical polybasic cleavage motif; thus, the mechanism of HA-mediated virulence remains unclear.

Structurally, the HA comprises two distinct regions: the globular head region bearing the receptor binding domain and major antigenic sites and the long, extended membrane-proximal stem bearing the fusion peptide (12). The HA can undergo cotranslational or posttranslational glycosylation modification by attaching oligosaccharides to the asparagine (Asn) side chain in N-X-(S/T) sequons (X represents any residue except proline). The structure and composition of glycans on the HA molecule surface are dependent largely on the accessibility of glycosylation sequons to saccharide-modifying enzymes provided by host cells, and a variety of glycans, including high mannose, complex type, and

TABLE 1 Pathogenicity of 1918 wild-type HA or glycan mutant recombinant viruses in mice

Virus	Introduced mutation(s)	Wt loss (%)[a] (10^5 PFU)	Wt loss (%)[a] (10^3 PFU)	LD$_{50}$[b]
1918-HA-WT:PR8	None	24.8	25	2.2
1918-HA+2G(142, 172)	E144T, G172N	25	24.9	2.0
1918-HA+2G(71, 286)	K71N, N73S, D286N, P288S	20	3.0	4.6
1918-HA+4G(71, 142, 172, 286)	K71N, N73S, E144T, G172N, D286N, P288S	22.6	4.4	5.5

[a] The percent mean maximum weight loss following 10^5 or 10^3 PFU inoculation.
[b] Fifty percent mouse lethal dose (LD$_{50}$) is expressed as the $\log_{10}$ PFU required to give one LD$_{50}$.

hybrid type, all have been found on HA molecules (13–15). Glyco-sylation of HA is essential for protein folding, and removal of key glycans at specific HA sites may result in improperly folded proteins, which are either degraded before transport to the cell surface or ac-cumulate in the Golgi complex (16, 17). However, not all of the gly-cosylation sites are crucial for HA folding and transport; some glyco-sylation sites are more involved in HA biological functions, including receptor binding activity, evasion of host immunity, and the HA cleavability (18). The presence of glycans in close proximity to the receptor binding domain (CRD) has been shown to modulate recep-tor binding affinity and specificity of influenza viruses of different subtypes by filling or masking the receptor binding domain (19, 20). Furthermore, the N-linked glycosylation sites on the HA molecule can interact with host carbohydrate binding proteins, mainly calci-um-dependent (C-type) lectins, and therefore affect host innate im-mune system recognition and the ability of the HA to induce adaptive immune response (21, 22).

The analysis of HA sequences of human H1N1 virus isolates from 1918 to 2010 has revealed a gradual increase in glycosylation sites, especially on the HA globular head region, ranging from one glycosylation site for the 1918 virus to four or five glycosylation sites for contemporary seasonal H1N1 viruses (23). Interestingly, the A(H1N1)pdm09 and 1918 viruses share the same number of glycosylation sites on the HA molecule (24). In the current study, we used the HA proteins from the 1918 virus and a seasonal (2006) H1N1 virus to determine the role of glycosylation in the H1 HA in viral pathogenicity and antigenicity. By adding or deleting HA glycosylation sites individually or in combination, we were able to identify specific sites responsible for virulence and antigenic prop-erties of H1N1 viruses.

MATERIALS AND METHODS

Cells, viruses, and plasmids. Madin-Darby canine kidney (MDCK) cells and human embryonic kidney (293T) cells were maintained in Dulbecco's modified Eagle's medium (DMEM) with 10% fetal bovine serum (FBS) as previously described (25). The human bronchial epithelial cell line, Calu-3, obtained from American Type Culture Collection (ATCC; Ma-nassas, VA), was grown in Eagle's minimal essential medium (MEM) supplemented with 10% FBS (25). Calu-3 cells were grown on transwells and allowed to polarize before inoculation of virus (26). The HA gene of A/Solomon Island/2006 (SI/06) H1N1 virus was cloned into the bidirec-tional pDZ vector as described previously (27). The plasmid DNA encod-ing the HA gene from A/South Carolina/1/1918 (1918 SC) in one direc-tional reverse genetic vector pPolI has been previously described (9). The Agilent QuikChange site-directed mutagenesis kit (Santa Clara, CA) was used to introduce mutations into pDZ-SI/06-HA or pPolI-1918-HA at desired sites (shown in Tables 1 and 2). A set of plasmids encoding indi-vidual segments of A/Puerto Rico/8/1934 (PR8) virus in pDZ vector for virus rescue was kindly provided by Adolfo García-Sastre, Mount Sinai School of Medicine, New York, NY. The sequences of wild-type (WT) and mutant HAs and subsequent rescued viruses were confirmed by sequenc-

ing to ensure no inadvertent mutations were introduced during the mu-tagenesis.

Rescue of PR8 recombinant viruses with the HA genome segment from the SI/06 or 1918 virus. The recombinant viruses containing WT and mutant HA genes of SI/06 or 1918 virus generated on a PR8 backbone (7 plasmids encoding pDZ-PR8 PB1, PB2, PA, NP, M, NS, and NA) were rescued as described previously (9). Plaque-purified viruses were ampli-fied by 2 to 3 passages in MDCK cells to prepare virus stocks. For SI/06-Δ1G104 and SI/06-Δ3G (71, 142, 177) mutant viruses, which failed to form plaques efficiently in MDCK cells, the 293T cell supernatants from the transfected cells were passaged twice in eggs before being amplified once in MDCK cells for making virus stocks. The rescue of 1918-HA:PR8 recombinant viruses was conducted under biosafety level 3 containment, including enhancements as outlined in *Biosafety in Microbiological and Biomedical Laboratories* (http://www.cdc.gov/biosafety/publications /bmbl5/).

Biotinylation of surface proteins and immunoprecipitation. 293T cells were transfected with pDZ-SI/06-HA of WT or mutant forms for detecting SI/06 HA surface expression. Similarly, cells were transfected with pPolI-1918-HA of WT or mutant forms plus pDZ-PR8-PB1, -PB2, -PA, and -NP encoding the influenza polymerase complex for detecting 1918 HA surface expression. The transfected cells were incubated with trypsin (0.5 μg/ml) for 30 min at 37°C to cleave HA0 before biotinylation was performed. The surface proteins of transfected 293 T cells were then biotinylated and immunoprecipitated using NeutrAvidin agarose resin (Pierce Biotechnology, Rockford, IL) according to established methods (28). The surface-expressed HA protein was analyzed by Western blotting using mouse anti-H1 HA monoclonal antibody (08-0172 recognizes a linear epitope within HA2) kindly provided by Xiyan Xu at the Centers for Disease Control and Prevention.

Mouse inoculations. All animal experiments were performed under the guidance of the Centers for Disease Control and Prevention's Institu-tional Animal Care and Use Committee and were conducted in an Asso-ciation for Assessment and Accreditation of Laboratory Animal Care In-ternational-accredited animal facility. Female BALB/c mice (Charles River Laboratories, Wilmington, MA), 6 to 8 weeks old, were inoculated intranasally (i.n.) with 50 μl of phosphate-buffered saline (PBS)-diluted

TABLE 2 Pathogenicity of SI/06 wild-type HA or glycan mutant recombinant viruses in mice

Virus	Introduced mutation(s)	Wt loss (%)[a] (10^5 PFU)	LD$_{50}$[b]
SI/06-HA-WT:PR8	None	6.2	>6
SI/06-Δ2G(142,177):PR8	N142K, N177I	25	3.5
SI/06-Δ1G142:PR8	N142K	9.9	5.6
SI/06-Δ1G177:PR8	N177I	23.7	3.4
SI/06-Δ1G71:PR8	N71K	5.7	>6
SI/06-Δ1G104:PR8	N104A	10.8	>6
SI/06-Δ3G(71, 142, 177):PR8	N71K, N142K, N177I	14.4	4.2

[a] The percent mean maximum weight loss following 10^5 or 10^3 PFU inoculation.
[b] Fifty percent mouse lethal dose (LD$_{50}$) is expressed as the $\log_{10}$ PFU required to give one LD$_{50}$.

virus following anesthesia with 0.2 ml of 2,2,2-tribromoethanal in tert-amyl alcohol (Avertin; Aldrich Chemical Co., Milwaukee, WI). The 50% lethal dose (LD_{50}) was determined by inoculating groups of five mice i.n. with serial 10-fold dilutions of virus and was calculated using the statistical method of Reed and Muench (44). Whole mouse lungs were collected on days 3 ($n = 5$) and 5 ($n = 5$) postinoculation (p.i.) following inoculation of 10^3 PFU or 10^3 50% egg infective doses (EID_{50}) of the indicated viruses. In addition, whole brain and spleen tissues were collected on day 3 p.i. Tissue homogenates were prepared, and viral titers were determined by plaque assay in MDCK cells or in eggs (8, 9).

Virus infection and plaque assay. Human Calu-3 cells were cultured and infected as previously described (26). Briefly, polarized Calu-3 cells, grown on transwells, were inoculated apically with the indicated influenza viruses at a multiplicity of infection (MOI) of 0.01 for 1 h, washed, and incubated at 37°C in a 5% CO_2 atmosphere. Culture supernatants were collected at 2, 16, 24, 48, and 72 h p.i., and viral titers were determined in a standard plaque assay with MDCK cells.

HI assay. Individual serum samples were collected from 3 to 5 mice 21 days p.i. Mouse sera were pretreated with receptor-destroying enzyme (RDE) from *Vibrio cholerae* (Denka Seiken, Tokyo) overnight, followed by heat treatment (56°C, 30 min) (29). Hemagglutination inhibition (HI) assays were performed with 0.5% turkey red blood cells by standard methods, and the HI titer was determined by the reciprocal of the highest dilution of serum without agglutination.

Building HA1 glycoprotein forms of 1918 HA and SI/06 HA. Based on X-ray crystal structures of 1918 HA (PDB identifier 2WRG) and SI/06 HA (PDB identifier 3SM5), we generated structures of HA1 glycoproteins with a basic trimannosyl core structure added to the appropriate glycosylation sites (described in this study) using the GlyProt tool (http://www.glycosciences.de/modeling/glyprot/php/main.php). The complex of SI/06 with avian receptor was modeled by superimposing the HA1 of A/Puerto Rico/8/34 H1N1 HA cocrystallized with LSTa (PDB identifier 1RVX) with the HA1 of SI/06 HA. In the case of 1918 HA, the appropriate amino acid changes to introduce glycosylation sites were made using mutagenesis wizard in PyMol, and the modified structure was submitted to the GlyProt server to build the glycoprotein.

Dose-dependent direct binding of H1N1 virus by glycan array. A streptavidin plate array comprising representative biotinylated α2-3- and α2-6-sialylated glycans was used for the analysis (30, 31). The representative avian influenza virus receptors, 3′SLN-LN and 3′SLN-LN-LN, have a 3′SLN-terminal motif corresponding to the branch length of N- or O-linked glycan receptors and represent the physiologically presented glycan receptors in mice (30, 31). LN stands for lactosamine unit -Galβ1-4GlcNAcβ1-, LN-LN is two lactosamine units linked via β1-3 linkage, and SLN stands for sialyl-lactosamine, where 3′SLN corresponds to Neu5Acα2-3Galβ1-4GlcNAcβ1- and 6′SLN corresponds to Neu5Acα2-6Galβ1-4GlcNAcβ1-. The glycans 6′SLN and 6′SLN-LN are representative influenza virus receptors in the human airway (30, 31). The viruses (hemagglutination units [HAU]; titers indicated) were diluted to 250 μl with 1× PBS-1% bovine serum albumin (BSA). Diluted virus in 50 μl was added to each of the glycan-coated wells and incubated overnight at 4°C. The primary and secondary antibodies used to detect binding were ferret anti-1918 or anti-SI/06 antisera (1:500 diluted in 1× PBS-1% BSA) and anti-ferret horseradish peroxidase (HRP)-conjugated antibody (1:500 diluted in 1× PBS-1% BSA). After each step, the wells were washed twice with 1× PBST (1× PBS-0.1% Tween 20) followed by 1× PBS. The wells were blocked with 1× PBS-1% BSA for 2 h at 4°C before antibodies were added. The binding signals were determined based on the HRP activity, determined by using the Amplex red peroxidase assay (Invitrogen) according to the manufacturer's instructions. The assays were done in triplicate, and appropriate negative controls were included.

RESULTS

HA molecules of 1918 pandemic and seasonal human H1N1 influenza A viruses have distinct glycosylation patterns. The predicted N-linked glycosylation sequons [N-X-(S/T)] reveal that the 1918 virus has only one glycosylation site at amino acid (aa) Asn 104 (1918 numbering, starting at the first methionine [Met] position) on the HA (defined by the aa region 64 to 286), and crystallographic studies have confirmed clear N-linked glycosylation of Asn at aa position 104 (32). Structurally, Asn 104 is located on the side of the HA head in the vestigial esterase subdomain positioned below antigenic site Ca2 (Fig. 1). The majority of the 1918 H1N1 viral descendants, before their disappearance in 1957, gained a glycosylation site on the side of the HA head (Asn 286) located close to the boundary between the HA head and stem region. In addition, most 1918 H1N1 viral descendants acquired an extra glycosylation site on the top of the HA head at either position 142 (with amino acid variation at position 144) or 177 (with amino acid variation at position 172 or 179), with some viruses having two glycosylation sites, at both Asn 142 and 177. Antigenically, both Asn 142 and Asn 177 (or 172 and 179) are in the Sa site, adjacent to the receptor binding pocket. When the H1N1 subtype reemerged in 1977 and further evolved in humans, most of the subsequent human H1N1 viruses shared very similar glycosylation patterns, in which two glycans appeared on the top of the HA head, at Asn 144 and 177, and two glycans appeared on the side of the HA head, at Asn 104 and 286. Around 1987, H1N1 viruses acquired a glycan at Asn 71, located on the side of the HA head and in close proximity to Asn 104 (Fig. 1). This change shifted the glycan on the top of the HA head from aa position 144 to 142, and typical H1N1 viruses during that time period, as illustrated by A/H1N1/Texas/91 (Texas/91), possessed five glycans on the HA head (Fig. 1). Among the five glycans, three are attached to the side of the HA head at Asn 71, 104, and 286, and two glycans are positioned on the top of the HA head, attached to Asn 142 and 177. In the mid-1990s, there was a trend to lose the glycan at Asn 286, and prior to the emergence of the A(H1N1)pdm09 virus, the majority of H1N1 viruses possessed two glycans at 142 and 177 and two glycans at 71 and 104, represented by A/Solomon Island/2006 (SI/06) virus (Fig. 1, right).

Construction and characterization of recombinant viruses with altered glycosylation sites. We first examined whether removing existing or introducing new glycosylation sequons for SI/06 or 1918 HA, respectively, results in molecular weight changes (indicative of glycan modifications) of the corresponding HAs. For this purpose, we compared the HA protein expression levels on the surface of 293T cells following transfection of plasmids encoding either WT or mutant HAs. In general, SI/06 and 1918 HA glycan mutants expressed intensities of HA protein bands similar to those of their corresponding WT HAs (Fig. 2A and B). Compared to WT HA, single-glycan mutants of SI/06 HA at aa 71, 104, 142, or 177 migrated faster through the gel (Fig. 2A). Moreover, mutant HA proteins with two or three glycosylation sequons deleted displayed a slightly greater rate of migration through the gel than HA containing single-glycan mutants.

For 1918 HA, the slower migration rate of mutant HA than of WT 1918 HA indicated that glycans were added at either aa 142, 71, or 286 (Fig. 2B). When glycan mutants were generated at Asn 172, 177, or 179, only the glycan mutant at aa 172 showed slower mobility shift than 1918-HA-WT, but not the mutants at 177 or at
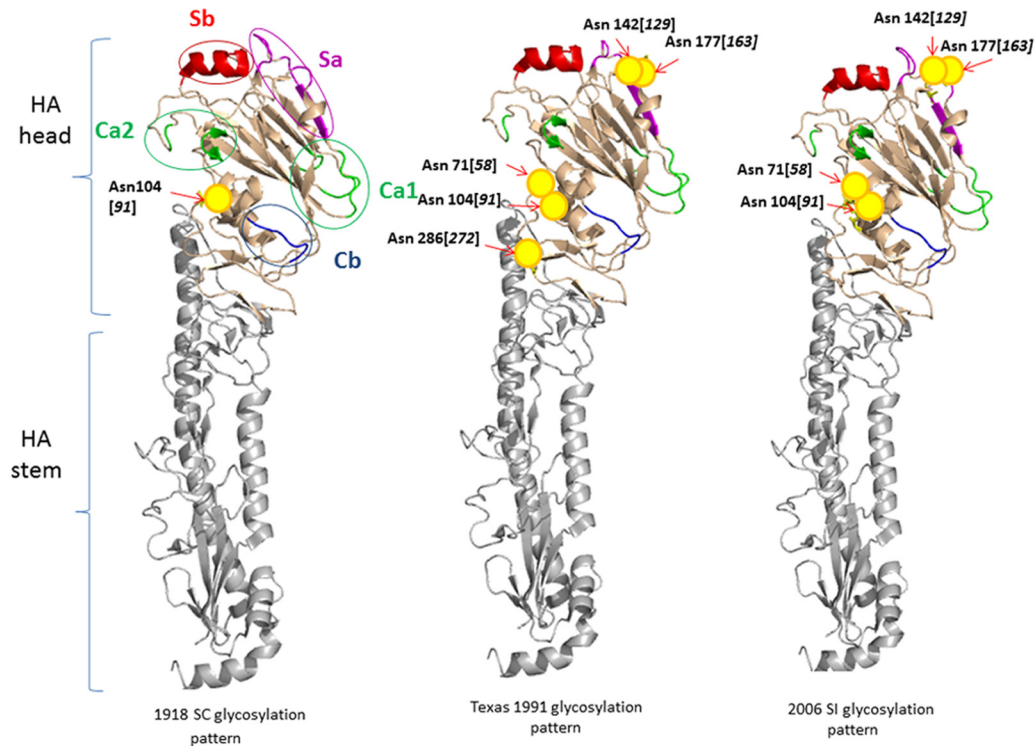
FIG 1 The glycosylation patterns of selective strains of human H1N1 viruses. Ribbon diagrams of monomeric H1 HA structures were illustrated with the PyMol program using 1918 SC HA0 as the template (PDB entry, 1RD8). The italicized numbers inside brackets are based on H1 HA crystal structure (1RUZ) numbering. The antigenic sites Sa, Sb, Ca, and Cb are colored in magenta, red, green, and blue, respectively. The potential glycosylation sites on the HA of 1918 SC, Texas/91, and SI/06 virus are shown in yellow circles, with the corresponding Asn labeled.

179 (Fig. 2B). Structurally, aa 172 is at the tip of a loop located on the top of the HA head, which would potentially have greater exposure to saccharide-modifying enzymes than glycans at aa positions 177 or 179. Therefore, the glycan mutant at position 172 was chosen over HA mutants at aa position 177 or 179 to construct double- or tetra-glycan mutants in subsequent studies. When four glycosylation sequons at positions 71, 142, 177, and 286 were introduced to 1918 HA simultaneously, the mutant HA migrated even slower than double mutants 1918-HA+2G(71, 286) and 1918-HA+2G(142, 172). Taken together, these results indicate that the glycosylation patterns in the HA head of H1N1 viruses can be altered with no apparent effect on protein folding and transport.

To further investigate the effect of HA glycosylation on the biological functions of H1 HA, recombinant viruses possessing the HA from SI/06 or 1918 or their glycan mutant forms were rescued on the seven-gene PR8 backbone, and viral replication kinetics were compared in human airway epithelial Calu-3 cells. In comparison to SI/06-HA-WT virus, the SI/06 recombinant virus with single-glycan deletion mutations on the top of the HA head at aa position 142 or 177 exhibited relatively similar growth kinetics, with a maximum 10-fold difference displayed by SI/06-Δ1G177 at one time point (24 h) only (Fig. 2C, left). The double-glycan deletion virus SI/06-Δ2G(142, 177) showed a moderate growth defect at early time points of 16 and 24 h p.i.; however, the difference in titers compared to those of the WT was narrowed after 24 h p.i., and the SI/06-Δ2G virus was able to reach a peak titer of over 10^8 EID$_{50}$/ml by 48 h.

In regard to SI/06-Δ1G71 and SI/06-Δ1G104 (side of the HA

head) glycan deletion mutants, we found that the SI/06-Δ1G71 virus replicated to a titer comparable to that of SI/06-HA-WT virus up to 24 h p.i., but the peak titer at 48 h p.i. was approximately 40-fold lower than that of the SI/06-HA-WT virus (Fig. 2C, right). The remaining single-glycan deletion mutant, SI/06-Δ1G104, and the SI/06-Δ3G(71, 142, 177) triple-glycan mutant displayed a significant growth defect at early time points compared to SI/06-HA-WT virus, but the differences in viral titers compared to those of the WT virus narrowed after 48 h p.i. Taken together, our results demonstrate that the glycans on the side of the HA head have a greater impact on SI/06 recombinant virus replication than the glycans on the top of the HA head.

The comparison of replication kinetics of 1918-HA-WT and glycan mutant viruses in human Calu-3 cells demonstrated that there were no significant differences in viral replication between the 1918 HA glycan mutant virus 1918-HA+2G(142, 172) and the 1918-HA-WT virus (Fig. 2D). However, the other double-glycan mutant virus, 1918-HA+2G(71, 286), displayed slower growth kinetics than the 1918-HA-WT virus for the first 48 h p.i. before returning to levels comparable to those of the other recombinant viruses at 72 h. Of interest, the tetra-glycan mutant virus 1918-HA+4G(71, 142, 172, 286), containing two glycans on the side (aa 71 and 286) and two glycans on the top (aa 142 and 172), replicated more efficiently than the double-glycan mutant virus 1918-HA+2G(71, 286) and showed a growth curve similar to that of the double-glycan mutant virus 1918-HA+2G(142, 172). These results demonstrate that adding extra glycans on the top of the 1918 HA head could partially compensate for the growth defects associated with adding two glycans on the side of the HA.
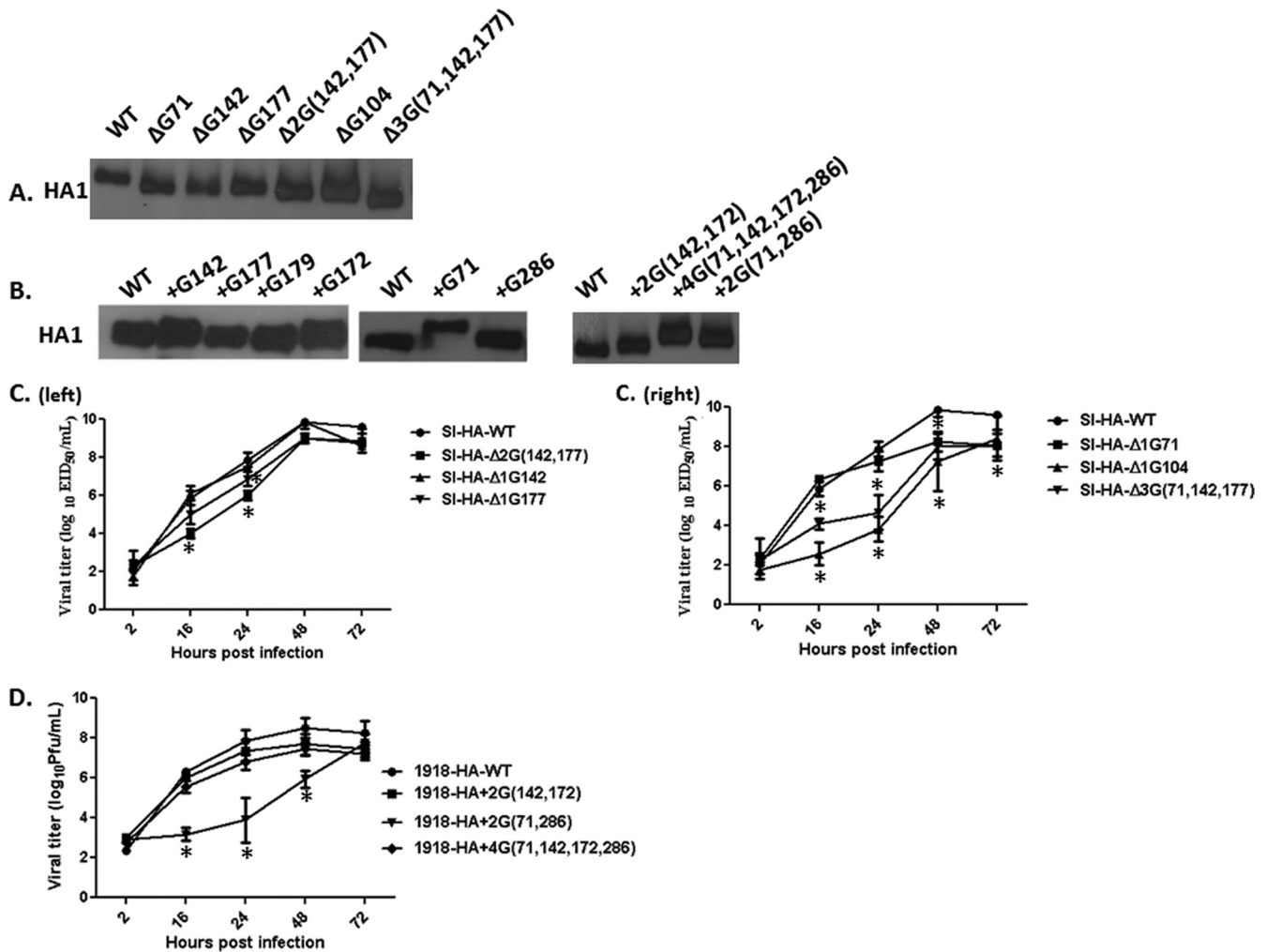
FIG 2 The effect of mutating glycosylation sites on the HA molecular weight and growth kinetics of SI/06 and 1918 HA recombinant viruses. The surface expression of WT or glycan mutant forms of SI/06 HA (A) and 1918 HA (B) was examined by labeling surface proteins with sulfo-NHS-SS-biotin followed by immunoprecipitation with NeutrAvidin beads. The surface-expressed HAs were detected by Western blotting with anti-H1 HA antibody. Calu-3 cells were infected with the recombinant viruses bearing WT or glycan mutant HAs from SI/06 (C) or 1918 SC (D) virus at an MOI of 0.01 for 1 h, and the infected cell supernatants were collected at the indicated time points for viral titer determination. Error bars represent the standard deviation (SD) of the mean from three independent experiments. An asterisk indicates that the titers of the mutant viruses were significantly different from those of the WT virus at the indicated time points by two-way analysis of variance (ANOVA) test.

1918 recombinant viruses with additional glycans in the HA head are attenuated *in vivo*. To determine whether the high-virulent phenotype of the 1918 virus is due to the largely nongly-cosylated HA, we used mice to compare the virulence of the PR8 recombinant viruses possessing either the WT 1918 HA or glycan addition mutants. Consistent with previous studies (9), a single-gene 1918-HA-WT PR8 recombinant (1918-HA-WT) virus was highly lethal in mice, with an LD_{50} of $10^{2.2}$ (Table 1), and lung titers reached high titers of up to 10^6 PFU/ml on days 3 and 5 p.i. (Fig. 3A). The double-mutant virus 1918-HA+2G(142, 172), containing two glycans on the top of the HA head, was as virulent ($LD_{50} = 10^{2.0}$) in mice as the 1918-HA-WT virus. In contrast, the other double-mutant virus, 1918-HA+2G(71, 286), containing two glycans on the side of the HA head, was attenuated in mice and required approximately 300-fold more virus to kill half of the infected mice ($LD_{50} = 10^{4.6}$). At a lower virus inoculum (10^3 PFU), the mean maximum weight loss was <5%, and lung viral

titers were approximately 3 log units lower than those of the WT group both days p.i. (Table 1 and Fig. 3A). The quadruple-mutant virus 1918-HA+4G(71, 142, 172, 286), which shares the same glycosylation pattern as the seasonal Texas/91 H1N1 virus, was further attenuated ($LD_{50} = 10^{5.5}$) compared to the double-glycan mutant virus 1918-HA+2G(71, 286). Despite the increased attenuation of the 1918-HA+4G(71, 142, 172, 286) virus, the lung titers from these inoculated mice were about 2.5 and 1.6 log units higher than those from the double-glycan mutant 1918-HA+2G(71, 286)-infected mice at day 3 and day 5 p.i., respectively (Fig. 3A). The ability of the quadruple-mutant virus to replicate more efficiently than HA+2G(71, 286) in the mouse lung was consistent with its growth properties in the human Calu-3 cells. Systemic spread of infectious virus to the brain or spleen was not detected (day 3 p.i.) in any of the mice infected with the 1918-HA-WT virus or glycan addition mutant viruses (data not shown), indicating that the addition of glycosylation sites to the
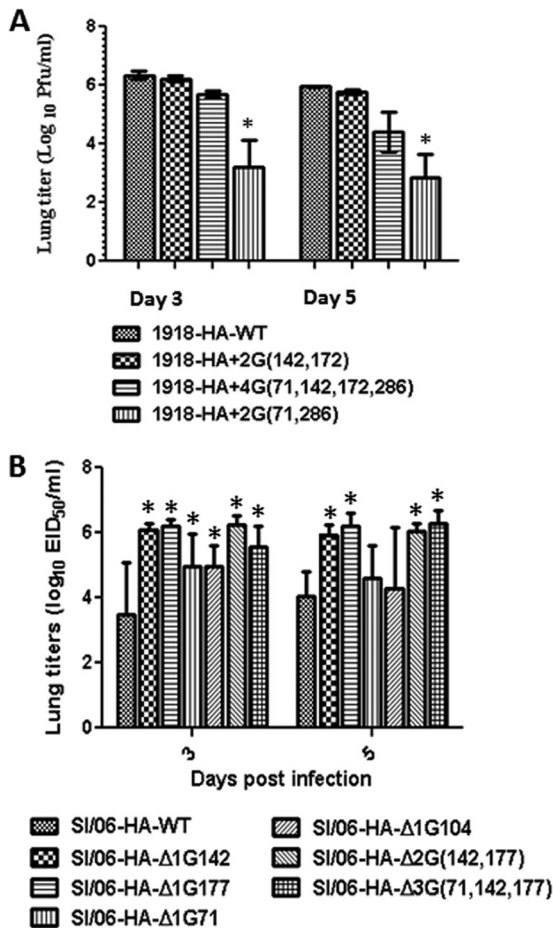
FIG 3 Glycan mutant virus infection in mice. Groups of BALB/c were inoculated i.n. with 10^3 PFU of the indicated 1918 (A) or SI/06 (B) recombinant viruses. Whole-lung tissues were isolated on days 3 ($n = 5$) and 5 ($n = 5$) p.i., and viral titers were determined by plaque assay in MDCK cells (expressed as mean $\log_{10}$ PFU/ml $\pm$ SD) (A) or in eggs (expressed as mean $\log_{10}$ EID$_{50}$/ml $\pm$ SD) (B). The asterisks indicate the lung titers were significantly different ($P < 0.05$) from those of the corresponding wild-type virus group by two-way ANOVA statistical analysis.

1918 HA did not alter the virus tissue tropism. Taken together, we demonstrated that the 1918-HA-WT virus could be effectively attenuated by simply adding two glycans on the side of the HA head and further attenuated by adding two additional glycans on the top of the HA head.

Removing glycosylation sites from seasonal influenza SI/06 HA enhances virulence *in vivo*. We next investigated whether removing glycans from SI/06 HA would affect the virulence of SI/06-HA-WT recombinant virus in the mouse model. Groups of mice were infected i.n. with 10-fold serial dilutions of PR8 recombinant viruses bearing WT SI/06 HA or HA with glycan mutations. For each virus group, additional mice ($n = 10$) were inoculated with 10^3 EID$_{50}$ of virus for assessing lung viral titers at two time points. As shown in Table 2, the PR8 recombinant virus with WT SI/06 HA was found to be nonlethal for BALB/c mice, who exhibited only modest weight loss (mean maximum weight loss = 6.2%), even at the highest inoculating dose of 10^6 EID$_{50}$. In stark contrast, the double-glycan mutant SI/06-HA-Δ2G(142, 177) caused 100% lethality at a dose of 10^5 EID$_{50}$ or higher with an

LD$_{50}$ = $10^{3.5}$. To further investigate the specific glycosylation site associated with the enhanced virulence, single-glycan mutant viruses were compared. Both single mutants, SI/06-HA-Δ1G142 and SI/06-HA-Δ1G177, were found to be lethal in mice, with LD$_{50}$ values of $10^{5.6}$ and $10^{3.4}$, respectively. SI/06-HA-Δ1G177 was as virulent as the SI/06-HA-Δ2G double mutant, suggesting that the glycan at aa position 177 plays a more dominant role in increasing virulence for SI/06-HA-WT virus.

In contrast to the phenotypic changes in mice following mutating glycosylation sites on the top of the HA head, the SI/06 glycan mutants (SI/06-HA-Δ1G71, SI/06-HA-Δ1G104) lacking one glycan on the side of the HA head failed to increase virulence compared to SI/06-HA-WT virus and were avirulent in mice at all infection doses tested. Mutating both glycans on the side of HA, SI/06-HA-Δ2G(71, 104), failed to generate a competent virus and was not tested in mice. The SI/06-HA-Δ3G(71, 142, 177) triple-glycan mutant, lacking one glycan on the side of the HA and two on the top of the HA head, was lethal in mice but was unable to further increase virulence compared to that of the SI/06-HA-Δ2G(142, 177) double-glycan mutant, based on the LD$_{50}$ values ($10^{4.2}$ versus $10^{3.5}$).

Comparison of viral titers showed, in general, higher levels of infectious virus in the lungs of mice inoculated with the SI/06 glycan mutants than the mice inoculated with the SI/06-HA-WT virus (Fig. 3B). Compared to SI/06-HA-WT-infected lungs, which had mean titers of $10^{3.5}$ EID$_{50}$/ml and $10^{4.0}$ EID$_{50}$/ml in lung tissues at day 3 and day 5, respectively, the SI/06-HA-Δ1G177 and SI/06-HA-Δ2G(142, 177) mutant viruses exhibited a 100-fold increase in lung viral titer ($>10^6$ EID$_{50}$/ml) on both days p.i. Of interest, the SI/06-HA-Δ1G142 single-glycan deletion mutant virus, which was less virulent than the SI/06-HA-Δ2G(142, 177) double-glycan mutant, appeared to replicate as efficiently as the double mutant in mouse lung tissues (Fig. 3B). Furthermore, although the mutant viruses with glycan deletion on the side of the HA head at aa 71 or 104 were as avirulent as SI/06-HA-WT virus, they displayed significantly higher (30-fold) lung titers at day 3 than that of the SI/06-HA-WT-infected mice. In summary, our results with SI/06-HA-WT and glycan mutant viruses in mice suggest that removing glycans from the HA head of seasonal H1N1 viruses enhances viral replication in mouse lungs regardless of the location of the glycosylation sites; however, only glycan deletions on the top of the HA head can change the phenotype of a nonlethal seasonal H1 recombinant virus to a virulent virus in mice.

Effect of HA glycosylation changes on glycan receptor binding properties of 1918 and SI/06 HA. Several studies have demonstrated that N-linked glycosylation at specific sites on the HA head affects glycan receptor binding (20, 30, 33–35). In an effort to understand the relationship of HA glycosylation patterns and its receptor binding, the binding properties of SI/06 and 1918 HA recombinant viruses were quantitatively characterized using a glycan array platform. In the case of 1918 HA, introduction of glycosylation sites at 71 (*58*) (italicized number represents X-ray structure numbering) and 286 (*272*) leads to a cluster of glycans at 71 (*58*) and 286 (*272*) and the conserved glycosylation site at 104 (*91*) in H1N1 HA (Fig. 4A). This glycan cluster is likely to affect the *220* loop via its interaction with the glycosylation at the 104 position. It was demonstrated previously that glycosylation at 104 (*91*) critically governs binding of 1918 HA to human receptors (α2→6 sialylated glycans) (30). Similarly, glycosylation at positions 142 (*129*) and 172 (*158*) leads to a cluster of glycans in close proximity to each other. Glycosylation at the 142 (*129*) site influences the *130*
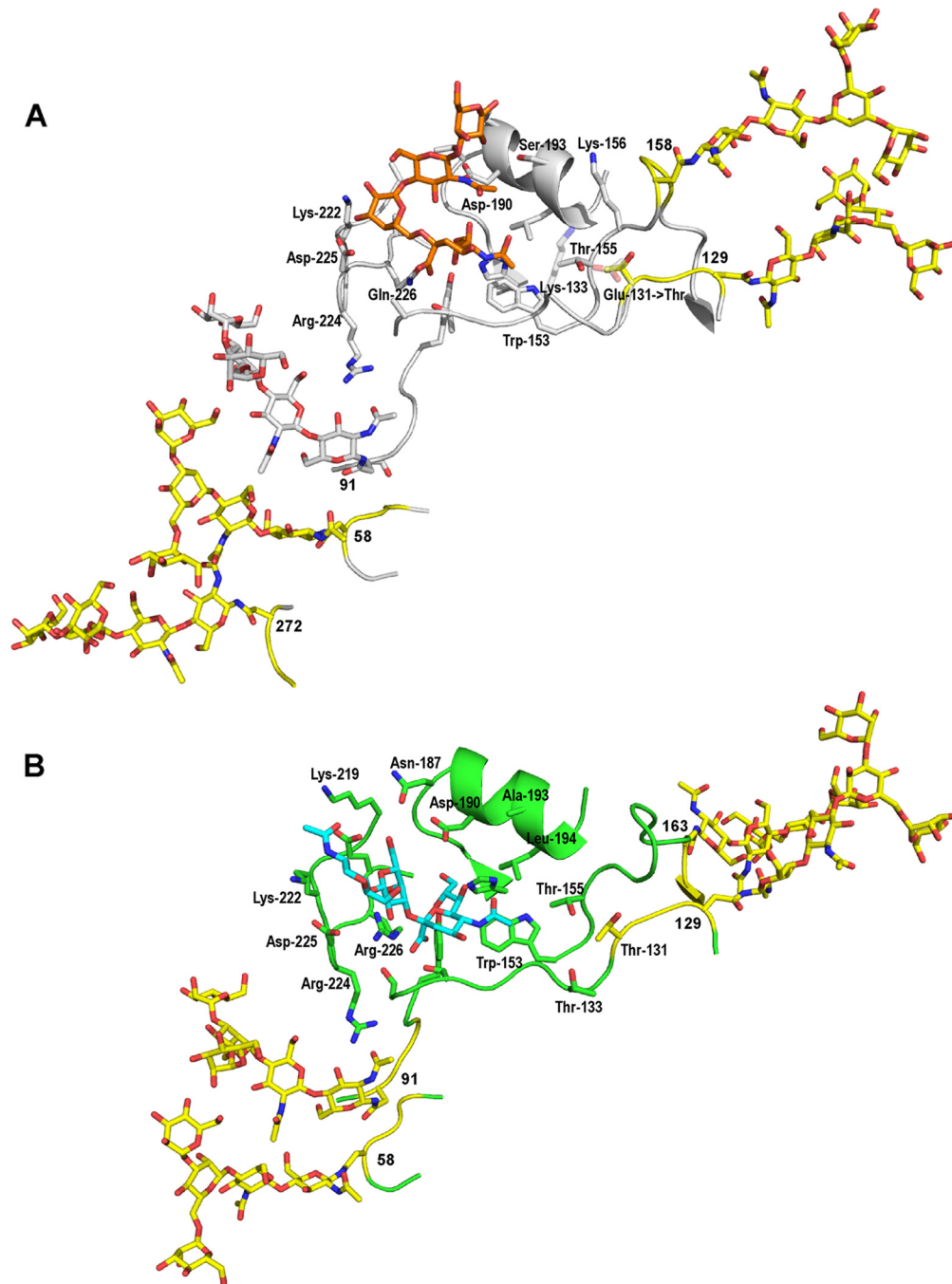
FIG 4 Structure of 1918 and SI/06 HA1 proteins. (A) 1918 HA1 with glycosylated sites 71, 104, 142, 172, and 286 in complex with human receptor. Shown in the figure is the glycan receptor binding site of 1918 HA, with key amino acids labeled (according to the numbering in the X-ray crystal structure) and their side chains shown. Glu *131* and Lys *133* side chains are shown at 50% transparency to highlight the change in interresidue interaction network when Glu *131* was mutated to Thr to add glycosylation site 142 in 1918 HA. The human receptor is shown, with the carbon atom colored orange. A basic trimannosyl core structure of an N-linked glycan is shown at the glycosylation sites 71 (*58*), 104 (*91*), 142 (*129*), 172 (*158*), and 286 (*272*). Among these sites, the glycosylation sites that were added through mutagenesis and their N-linked glycans are shown by the carbon atom colored yellow. (B) Structure of SI/06 HA HA1 with glycosylated sites 71, 104, 142, and 177 in complex with avian receptor. Shown in the figure is the glycan receptor binding site of SI/06 HA, where key amino acids are labeled (according to the numbering in the X-ray crystal structure) and their side chains are shown. The avian receptor is shown by the carbon atom colored cyan. A basic trimannosyl core structure of N-linked glycan is shown at the glycosylation sites 71 (*58*), 104 (*91*), 142 (*129*), and 177 (*163*), with the carbon atom colored yellow.

loop since Glu *131* is mutated to Thr, which affects the network of interresidue interactions involving Lys *133* and Thr *155*. Dose-dependent binding of the wild type and glycosylation site addition variants of 1918 HA using representative human receptors ($\alpha2\rightarrow6$

sialylated glycans) showed that adding the 1918-HA+2G(71, 286) or 1918-HA+2G(142, 172) glycan cluster, or simultaneously adding both glycan clusters, 1918-HA+4G(71, 142, 172, 286), had no significant effect on binding to long 6′SLN-LN (characteristic of
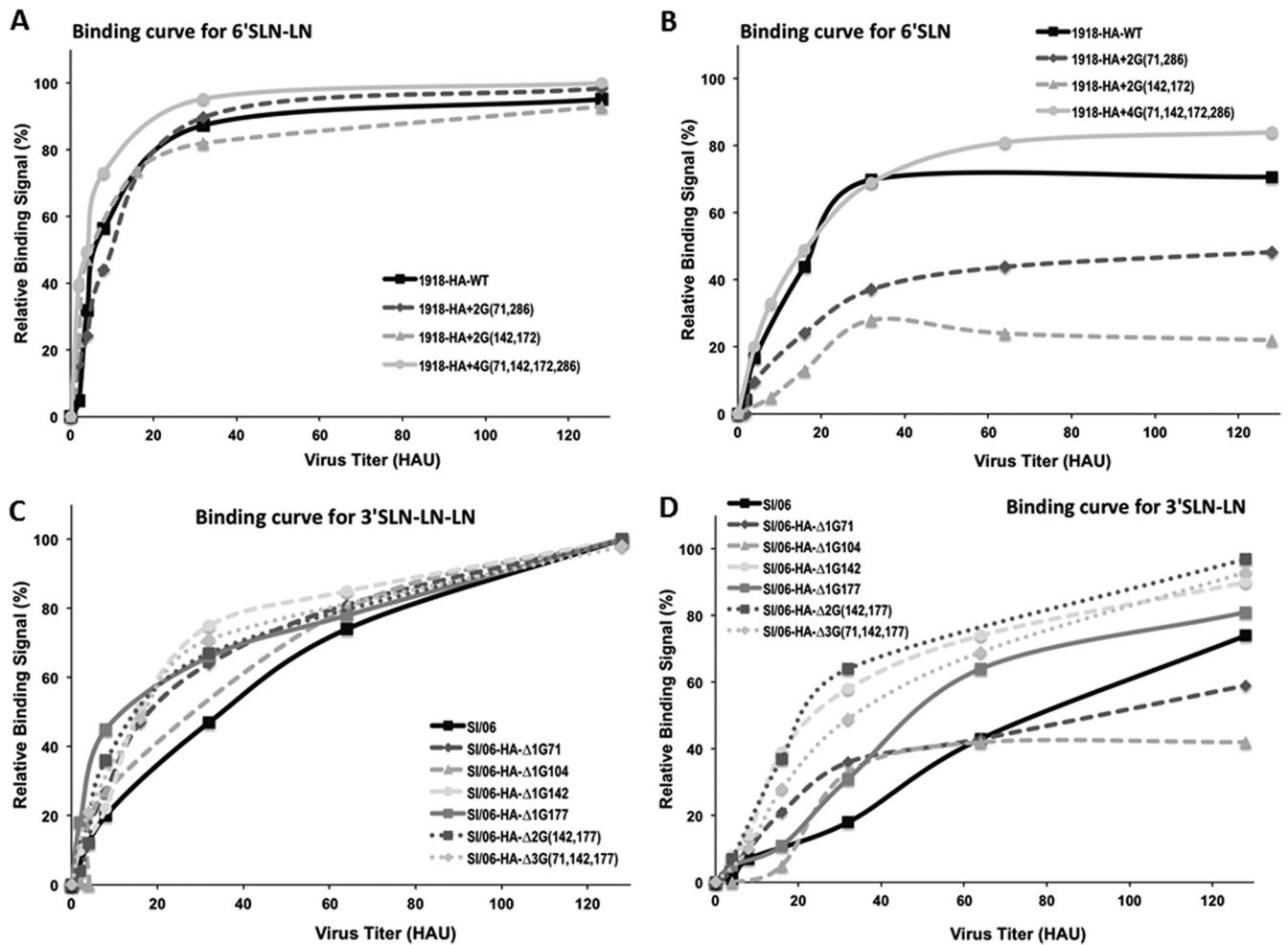
FIG 5 Dose-dependent glycan array binding of SI/06 and 1918 HA recombinant viruses. Dose-dependent binding of 1918 HA (A and B) or SI/06 HA (C and D) recombinant viruses representative of α2–3 and α2–6 sialylated glycans on the glycan array. The *y* axis shows percentage of maximum binding signal intensities.

human receptors) (Fig. 5A). However, both double-mutant viruses, 1918-HA+2G(71, 286) and 1918-HA+2G(142, 172), displayed reduced binding to short 6′SLN, whereas the binding avidity of the 1918-HA+4G(71, 142, 172, 286) quadruple-mutant virus was generally similar or marginally increased in comparison to that of the 1918-HA-WT virus (Fig. 5B).

Although SI/06 is a seasonal virus, the isolate used in this study (and also in the X-ray crystal structure) is an egg-adapted variant of the human H1N1 virus. The SI/06 HA used here has an Arg at position 226 (in contrast with Gln 226 typically present in human-adapted H1 HA), and it has been demonstrated previously that SI/06 virus with Arg 226 in HA predominantly binds to avian-like (α2–3) receptors (36). Structural analysis of glycosylation relative to the glycan receptor binding site of SI/06 HA (Fig. 4B) shows that glycosylation at 71 and 104 forms a cluster (similar to what was observed for 1918 HA), which is positioned to affect the *220* loop through interactions with glycosylation at position 104. Hence, removal of these sites, particularly at aa 104, is likely to affect glycan receptor binding through the *220* loop. Glycosylation at 142 and 177 is proximal to the *130* and *150* loop, respectively. Dose-dependent comparison binding of SI/06-HA-WT and glycan mutant viruses to the glycan array using representative avian

receptors (particularly to 3′SLN-LN-LN and 3′SLN-LN) showed no significant effect on binding to 3′SLN-LN-LN (Fig. 5C). However, the single-glycan mutant variants SI/06-Δ1G71 and SI/06-Δ1G104 (side of the HA head) displayed reduced binding to 3′SLN-LN in comparison to that of the SI/06-HA-WT virus (Fig. 5D). Conversely, single-glycan deletion mutations on the top of the HA head (SI/06-HA-Δ1G142 and SI/06-HA-Δ1G177) resulted in a modest increase in binding to 3′SLN-LN in comparison to that of the SI/06-WT-HA virus. Similarly, the double- and triple-glycan SI/06 HA mutants showed marginal increased 3′SLN-LN binding compared to that of the SI/06-HA-WT virus (Fig. 5D).

Altering glycosylation sites in the HA head of the SI/06 and 1918 pandemic viruses changes viral antigenicity. The HA globular head is the major target site of antibodies that neutralize viral infectivity. Using the HI assay, we next determined whether altering the glycosylation pattern in the HA head affects viral antigenicity. As shown in Fig. 6A, the SI/06-HA-WT mouse antisera could efficiently inhibit hemagglutination by not only homologous SI/06-HA-WT virus but also the four SI/06 HA glycan deletion mutants tested in this study. This suggests that the non-glycan-covered regions in the SI/06 HA head are the major antigenic
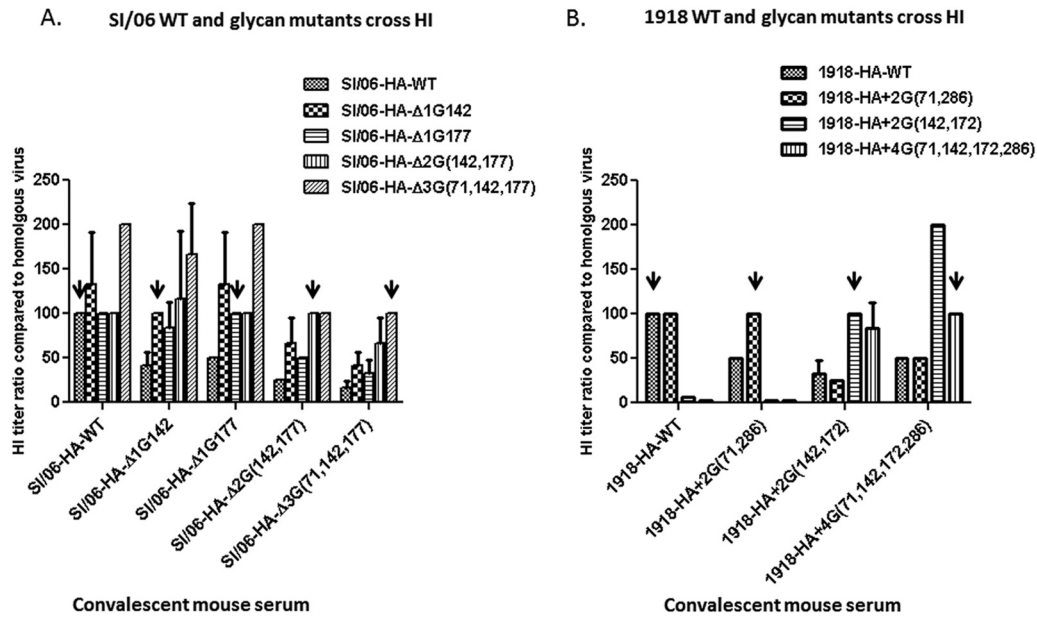
FIG 6 HI reactivity of antisera against SI/06-HA-WT, 1918-HA-WT, and glycan mutant viruses. HI assays were performed against both homologous and heterologous viruses, and the HI titer against homologous virus was normalized to 100% (indicated by the arrows). An HI titer of 160 or higher against homologous virus was obtained for all antisera collected. The average HI titers from three repeats are shown in the graph, and the error bars represent SD.

sites and the corresponding antibodies could recognize the WT as well as the glycan deletion mutants. Mouse antisera generated to single-glycan deletion mutants SI/06-HA-Δ1G142 and SI/06-HA-Δ1G177 displayed efficient HI reactivity for the glycan mutants, and HI titers against SI/06 WT virus were approximately 2-fold lower than that for the homologous mutant viruses. The HI reactivity against SI/06 WT virus was approximately 4-fold lower than that for the homologous mutant virus when the antisera against the double-glycan mutant SI/06-HA-Δ2G(142, 177) or triple-glycan mutant SI/06-Δ3G(71, 142, 177) were used. These results suggest that removing glycans on the top of the SI/06 HA head exposes antibody epitopes which are masked in the glycosylated form of the SI/06 HA.

The same assay was used to evaluate antigenicity of 1918 HA glycan mutants. The antisera against 1918-HA-WT virus could inhibit hemagglutination of the homologous virus and the double-mutant virus 1918-HA+2G(71, 286), containing two glycans on the side of the HA head, but showed very little or no HI reactivity against mutant viruses 1918-HA+2G(142, 177) and 1918-HA+4G(71, 142, 172, 286) (Fig. 6B). Antisera generated against 1918-HA+2G(71, 286) displayed an HI reactivity profile similar to that of 1918-HA-WT virus antisera, with a 2-fold-lower HI titer for the 1918-HA-WT virus but again only minimal HI titers against mutant viruses 1918-HA+2G(142, 172) and 1918-HA+4G(71, 142, 172, 286). Conversely, in general, antisera to the mutant viruses 1918-HA+2G(142, 172) and 1918-HA+4G(71, 142, 172, 286) showed a broader cross-reactive HI activity than 1918-HA-WT, and the antiserum against 1918-HA+4G(71, 142, 172, 286) showed the greatest cross-reactive HI activity against the 1918-HA+2G(142, 172) virus. Taken together, the results from our cross-reactive HI assays suggest that the major epitopes of the 1918-HA-WT virus exist in regions that can be covered by glycans attached at aa 142 and 172 and as a result can efficiently block antibodies from binding to the HA head.

DISCUSSION

After reconstruction of the 1918 pandemic influenza virus, its exceptionally high virulence was confirmed in the mouse, ferret, and nonhuman primate animal models (8, 9). Further characterization of 1918 recombinant viruses in mice and human airway cells revealed that the 1918 HA gene is essential for virulence and maximum virus replication of this pandemic strain (8, 9). Because the influenza HA has multiple functions in the viral life cycle, it has been difficult to unravel the precise virulence-associated function of this protein. In this study, we demonstrated for the first time that the low number of N-linked 1918 HA glycosylation sites directly contributes to its virulence in mice. Conversely, the avirulent phenotype of a recombinant 2006 seasonal H1N1 virus can be rendered virulent in mice by removing glycosylation sites on the top of the H1 HA molecule. In addition to influencing the phenotype of these viruses, glycosylation sites on the HA globular head were found to be critical for antigenicity of the H1N1 viruses and receptor binding activity of the seasonal SI/06 virus.

The numbers and locations of N-linked glycosylation sites on the HA protein vary with influenza subtype and strain (37). Our analysis and other published reports show that during influenza A virus evolution in humans, both the H1N1 and H3N2 subtypes have, with time, steadily acquired additional potential HA glycosylation sites (37). The acquisition of N-linked glycosylation sites on the HA protein is thought to play a beneficial role for the virus by shielding antigenic sites from interaction with antibodies. However, the consequence of increased HA glycosylation is the attenuation of human H1N1 and H3N2 influenza viruses that originated from pandemic viruses. In mice, H3N2 viruses bearing high levels of glycosylation displayed an attenuated virulence and were more sensitive to neutralization by the murine lung surfactant protein (SP-D) (38). SP-D belongs to the collectin family, which is a class of major carbohydrate binding proteins of the

innate immune system that selectively and preferentially recognize glycans with terminal mannose. By interacting with high-mannose oligosaccharides on the HA and the NA of influenza virus, SP-D can inhibit hemagglutination and NA activity, resulting in virus aggregation and inhibition of infectivity (38). For the H1N1 subtype, a recent study showed that A/Brazil/11/78 virus containing potential HA glycosylation sites at Asn 104, 144, 172, and 177 became less sensitive to SP-D neutralization and more virulent in mice when the glycosylation site at 144 was removed (39). This suggests that the glycan at aa 144 of the H1 HA was responsible mainly for SP-D binding and decreased susceptibility to SP-D inhibition resulting in enhanced virulence. In our study, we found that the glycan at Asn 177 of SI/06 H1N1 virus plays a dominant role in modulating virulence. In both studies, glycans at 144 and 177, which are located in close proximity to one another, played a critical role in attenuating virulence, possibly due to the increased sensitivity to SP-D neutralization. Whether the glycan at aa position 177 on the SI/06 HA head binds to SP-D and contributes to viral sensitivity to SP-D was not addressed in the current study and requires future examination.

Interestingly, we found in our study that the high virulence of the recombinant H1N1 virus possessing the 1918 HA could be attenuated only by adding two glycans on the side of the HA head (aa positions 71 and 286) but not by adding glycans on the top of the glycoprotein. This effect may be due, at least in part, to the capacity of early human H1N1 viruses to interact with SP-D preferentially via the glycans on the side of the HA head. It has been suggested that A/WSN/33 (H1N1), a variant of the first human influenza virus, possessing a high-mannose-type glycan buried in the HA trimer interface (aa 73 based on 1918 HA numbering), is capable of binding to SP-D (13–15). Conversely, the glycans at the remaining WSN/33 HA sites, including the glycans on the top of the HA head, are mainly complex-type sugar residues mostly terminating in galactose and incapable of binding to SP-D.

The present study also demonstrated that removal of glycosylation sites from SI/06 HA or adding glycosylation sites to 1918 HA led to distinct glycan binding properties. Although altered receptor binding affinity might affect pathogenesis *in vivo* (31, 40), in our study the changes in receptor binding avidity associated with acquiring or losing glycosylation sites in H1 viruses does not directly correlate with virulence. While some of the single-glycan mutants of SI/06 HA (specifically at 71 or 104) lowered receptor binding at high HAU concentrations, the double- and triple-glycan mutant viruses showed marginal increases in receptor binding avidity. Our results are consistent with the previous study with H5N1 virus, in which the systematic truncation of N-glycan structure resulted in the increased binding to avian-like ($\alpha2$–3) receptors, further suggesting that the presence of bulky glycans adjacent to receptor binding sites is able to hinder the avidity of virus binding to certain types of sialic acid (36). In the case of 1918 HA, the addition of glycosylation sites in the variants containing two glycans on the top of the HA head [1918-HA+2G(142, 172)] or on the side of the HA head [1918-HA+2G(71, 286)] led to lower binding to the short oligosaccharide (6′SLN) branch, with the 1918-HA+2G(142, 172) mutant showing the most reduction. Interestingly, a virus mutant with all four glycan mutations, 1918-HA+4G(71, 142, 172, 286), compensated for the diminished receptor binding and for the replication inefficiency brought about by the 1918-HA+2G(71, 286) mutation. Although the mechanism to explain improved viral fitness by adding additional glyco-

sylation sites remains unclear, the glycosylation at these sites impinges on the *220* and *130* loops that are involved in binding to glycan receptors.

The ability of glycosylation to sterically block antibody binding to HA and thus provide protection against the host immune response has been clearly demonstrated for influenza viruses (41–43). Using recombinant H1 viruses harboring various glycosylation forms of HA, we demonstrated that the antibodies induced by viruses with a high number of glycosylation sites have a broader neutralizing activity than the antibodies induced by the viruses with fewer glycosylation sites. This suggests that choosing a virus partially shielded by glycans on the HA head as a vaccine candidate can provide certain advantages in protecting against infection with viral variants with differing glycosylation patterns. However, whether such virus vaccines are equally immunogenic as their counterparts containing fewer glycosylation sites needs to be determined in the future.

Since the demonstration that the HA virus gene is essential for maximal replication and virulence of the 1918 virus, questions have been raised concerning the precise mechanism of action of this molecule. Although the HA contributes multiple functions to the virus, it is clear that the lack of 1918 HA glycosylation contributes to virulence in mice and replication in human airway cells. Moreover, glycosylation can affect the pattern of antigenic variation. Further study is needed to better understand the host response to infection with HA glycosylated variants, especially their interaction with human SP-D and opsonization mediated by SP-D. Taken together, this work underscores the importance of studying the contribution of N-linked glycosylation of the HA protein to virulence and antigenicity of influenza viruses. Knowledge of such molecular features that influence virulence and antigenicity would help identify emerging influenza viruses with the potential for heightened public health impact.

ACKNOWLEDGMENTS

REFERENCES

1. **Cox NJ, Subbarao K.** 2000. Global epidemiology of influenza: past and present. Annu. Rev. Med. **51:**407–421.
2. **Johnson NP, Mueller J.** 2002. Updating the accounts: global mortality of the 1918–1920 "Spanish" influenza pandemic. Bull. Hist. Med. **76:**105–115.
3. **Zimmer SM, Burke DS.** 2009. Historical perspective—emergence of influenza A (H1N1) viruses. N. Engl. J. Med. **361:**279–285.
4. **Maurizi CP.** 1985. Why was the 1918 influenza pandemic so lethal? The possible role of a neurovirulent neuraminidase. Med. Hypotheses **16:**1–5.
5. **Morens DM, Taubenberger JK, Harvey HA, Memoli MJ.** 2010. The 1918 influenza pandemic: lessons for 2009 and the future. Crit. Care Med. **38:**e10–e20.
6. **Neumann G, Kawaoka Y.** 2011. The first influenza pandemic of the new millennium. Influenza Other Respi. Viruses **5:**157–166.
7. **Centers for Disease Control and Prevention.** 2010. Update: influenza activity—United States, August 30, 2009-March 27, 2010, and composition of the 2010-11 influenza vaccine. MMWR. Morbid. Mortal. Wkly. Rep. **59:**423–430.
8. **Kobasa D, Takada A, Shinya K, Hatta M, Halfmann P, Theriault S, Suzuki H, Nishimura H, Mitamura K, Sugaya N, Usui T, Murata T, Maeda Y, Watanabe S, Suresh M, Suzuki T, Suzuki Y, Feldmann H,**

Kawaoka Y. 2004. Enhanced virulence of influenza A viruses with the haemagglutinin of the 1918 pandemic virus. Nature **431**:703–707.

9. Pappas C, Aguilar PV, Basler CF, Solorzano A, Zeng H, Perrone LA, Palese P, Garcia-Sastre A, Katz JM, Tumpey TM. 2008. Single gene reassortants identify a critical role for PB1, HA, and NA in the high virulence of the 1918 pandemic influenza virus. Proc. Natl. Acad. Sci. U. S. A. **105**:3064–3069.

10. Steinhauer DA. 1999. Role of hemagglutinin cleavage for the pathogenicity of influenza virus. Virology **258**:1–20.

11. Kawaoka Y, Webster RG. 1988. Sequence requirements for cleavage activation of influenza virus hemagglutinin expressed in mammalian cells. Proc. Natl. Acad. Sci. U. S. A. **85**:324–328.

12. Wilson IA, Skehel JJ, Wiley DC. 1981. Structure of the haemagglutinin membrane glycoprotein of influenza virus at 3 A resolution. Nature **289**:366–373.

13. Nakamura K, Bhown AS, Compans RW. 1980. Glycosylation sites of influenza viral glycoproteins. Tryptic glycopeptides from the A/WSN (H0N1) hemagglutinin glycoprotein. Virology **107**:208–221.

14. Keil W, Niemann H, Schwarz RT, Klenk HD. 1984. Carbohydrates of influenza virus. V. Oligosaccharides attached to individual glycosylation sites of the hemagglutinin of fowl plague virus. Virology **133**:77–91.

15. Schwarzer J, Rapp E, Hennig R, Genzel Y, Jordan I, Sandig V, Reichl U. 2009. Glycan analysis in cell culture-based influenza vaccine production: influence of host cell line and virus strain on the glycosylation pattern of viral hemagglutinin. Vaccine **27**:4325–4336.

16. Roberts PC, Garten W, Klenk HD. 1993. Role of conserved glycosylation sites in maturation and transport of influenza A virus hemagglutinin. J. Virol. **67**:3048–3060.

17. Gallagher PJ, Henneberry JM, Sambrook JF, Gething MJ. 1992. Glycosylation requirements for intracellular transport and function of the hemagglutinin of influenza virus. J. Virol. **66**:7136–7145.

18. Klenk HD, Wagner R, Heuer D, Wolff T. 2002. Importance of hemagglutinin glycosylation for the biological functions of influenza virus. Virus Res. **82**:73–75.

19. Abe Y, Takashita E, Sugawara K, Matsuzaki Y, Muraki Y, Hongo S. 2004. Effect of the addition of oligosaccharides on the biological activities and antigenicity of influenza A/H3N2 virus hemagglutinin. J. Virol. **78**:9605–9611.

20. Ohuchi M, Ohuchi R, Feldmann A, Klenk HD. 1997. Regulation of receptor binding affinity of influenza virus hemagglutinin by its carbohydrate moiety. J. Virol. **71**:8377–8384.

21. Geijtenbeek TB, Gringhuis SI. 2009. Signalling through C-type lectin receptors: shaping immune responses. Nat. Rev. Immunol. **9**:465–479.

22. Vigerust DJ, Shepherd VL. 2007. Virus glycosylation: role in virulence and immune interactions. Trends Microbiol. **15**:211–218.

23. Sun S, Wang Q, Zhao F, Chen W, Li Z. 2011. Glycosylation site alteration in the evolution of influenza A (H1N1) viruses. PLoS One **6**:e22844. doi:10.1371/journal.pone.0022844.

24. Igarashi M, Ito K, Yoshida R, Tomabechi D, Kida H, Takada A. 2010. Predicting the antigenic structure of the pandemic (H1N1) 2009 influenza virus hemagglutinin. PLoS One **5**:e8553. doi:10.1371/journal.pone.0008553.

25. Zeng H, Goldsmith C, Thawatsupha P, Chittaganpitch M, Waicharoen S, Zaki S, Tumpey TM, Katz JM. 2007. Highly pathogenic avian influenza H5N1 viruses elicit an attenuated type I interferon response in polarized human bronchial epithelial cells. J. Virol. **81**:12439–12449.

26. Zeng H, Pappas C, Katz JM, Tumpey TM. 2011. The 2009 pandemic H1N1 and triple-reassortant swine H1N1 influenza viruses replicate efficiently but elicit an attenuated inflammatory response in polarized human bronchial epithelial cells. J. Virol. **85**:686–696.

27. Hoffmann E, Krauss S, Perez D, Webby R, Webster RG. 2002. Eight-plasmid system for rapid generation of influenza virus vaccines. Vaccine **20**:3165–3170.

28. Sun X, Tse LV, Ferguson AD, Whittaker GR. 2010. Modifications to the hemagglutinin cleavage site control the virulence of a neurotropic H1N1 influenza virus. J. Virol. **84**:8683–8690.

29. Stephenson I, Wood JM, Nicholson KG, Zambon MC. 2003. Sialic acid receptor specificity on erythrocytes affects detection of antibody to avian influenza haemagglutinin. J. Med. Virol. **70**:391–398.

30. Jayaraman A, Koh X, Li J, Raman R, Viswanathan K, Shriver Z, Sasisekharan R. 2012. Glycosylation at Asn91 of H1N1 haemagglutinin affects binding to glycan receptors. Biochem. J. **444**:429–435.

31. Belser JA, Jayaraman A, Raman R, Pappas C, Zeng H, Cox NJ, Katz JM, Sasisekharan R, Tumpey TM. 2011. Effect of D222G mutation in the hemagglutinin protein on receptor binding, pathogenesis and transmissibility of the 2009 pandemic H1N1 influenza virus. PLoS One **6**:e25091. doi:10.1371/journal.pone.0025091.

32. Stevens J, Corper AL, Basler CF, Taubenberger JK, Palese P, Wilson IA. 2004. Structure of the uncleaved human H1 hemagglutinin from the extinct 1918 influenza virus. Science **303**:1866–1870.

33. Kasson PM, Pande VS. 2008. Structural basis for influence of viral glycans on ligand binding by influenza hemagglutinin. Biophys. J. **95**:L48–L50.

34. Stevens J, Blixt O, Chen LM, Donis RO, Paulson JC, Wilson IA. 2008. Recent avian H5N1 viruses exhibit increased propensity for acquiring human receptor specificity. J. Mol. Biol. **381**:1382–1394.

35. Wang CC, Chen JR, Tseng YC, Hsu CH, Hung YF, Chen SW, Chen CM, Khoo KH, Cheng TJ, Cheng YS, Jan JT, Wu CY, Ma C, Wong CH. 2009. Glycans on influenza hemagglutinin affect receptor binding and immune response. Proc. Natl. Acad. Sci. U. S. A. **106**:18137–18142.

36. Xu Q, Wang W, Cheng X, Zengel J, Jin H. 2010. Influenza H1N1 A/Solomon Island/3/06 virus receptor binding specificity correlates with virus pathogenicity, antigenicity, and immunogenicity in ferrets. J. Virol. **84**:4936–4945.

37. Cherry JL, Lipman DJ, Nikolskaya A, Wolf YI. 2009. Evolutionary dynamics of N-glycosylation sites of influenza virus hemagglutinin. PLoS Curr. **18**:RRN1001. doi:10.1371/currents.RRN1001.

38. Reading PC, Tate MD, Pickett DL, Brooks AG. 2007. Glycosylation as a target for recognition of influenza viruses by the innate immune system. Adv. Exp. Med. Biol. **598**:279–292.

39. Tate MD, Brooks AG, Reading PC. 2011. Specific sites of N-linked glycosylation on the hemagglutinin of H1N1 subtype influenza A virus determine sensitivity to inhibitors of the innate immune system and virulence in mice. J. Immunol. **187**:1884–1894.

40. O'Donnell CD, Vogel L, Wright A, Das SR, Wrammert J, Li GM, McCausland M, Zheng NY, Yewdell JW, Ahmed R, Wilson PC, Subbarao K. 2012. Antibody pressure by a human monoclonal antibody targeting the 2009 pandemic H1N1 virus hemagglutinin drives the emergence of a virus with increased virulence in mice. mBio **3**(3):e00120–12. doi:10.1128/mBio.00120-12.

41. Manicassamy B, Medina RA, Hai R, Tsibane T, Stertz S, Nistal-Villan E, Palese P, Basler CF, Garcia-Sastre A. 2010. Protection of mice against lethal challenge with 2009 H1N1 influenza A virus by 1918-like and classical swine H1N1 based vaccines. PLoS Pathog. **6**:e1000745. doi:10.1371/journal.ppat.1000745.

42. Wei CJ, Boyington JC, Dai K, Houser KV, Pearce MB, Kong WP, Yang ZY, Tumpey TM, Nabel GJ. 2010. Cross-neutralization of 1918 and 2009 influenza viruses: role of glycans in viral evolution and vaccine design. Sci. Transl. Med. **2**:24ra21.

43. Skehel JJ, Wiley DC. 2000. Receptor binding and membrane fusion in virus entry: the influenza hemagglutinin. Annu. Rev. Biochem. **69**:531–569.

44. Reed LJ, Muench H. 1938. A simple method of estimating fifty percent endpoints. J. Hygiene **27**:493–497.